ISBN: 978-3-95450-247-9 ISSN: 2673-5490 doi: 10.18429/JACoW-IPAC2024-WEPG16

MAGNETRON DIAGNOSTICS WITH A NOVEL OPTICAL FIBRE-CHERENKOV DETECTOR *

A. Jones[1†], J. Wolfenden[1], C. P. Welsch[1], University of Liverpool, UK
P. Abel, M. Mineo, N. O'Sullivan, Teledyne e2v, Chelmsford, UK
[1]also at Cockcroft Institute, Daresbury, UK

Abstract

Development of an optical fibre-based beam loss monitor (OBLM) is in progress at the Cockcroft Institute (CI), UK. The novel sensor utilizes the Cherenkov radiation (CR) emitted in optical fibres by relativistic particle showers generated in beam loss or breakdown events. Breakdowns are a problem for high-power magnetrons, such as those in medical accelerator facilities, as damage to the magnetron cathode reduces the device's efficiency and lifetime. These events can be detected by emitted CR channelled along the fibres to photomultiplier detectors, and a time-of-flight method can be used to calculate the breakdown location from the CR arrival time. This has previously been demonstrated with the OBLM system on RF cavities (at CLARA, Daresbury Laboratory, and CTF3, CERN) and allows for rapid and reliable breakdown detection, which is important for damage mitigation. This contribution presents proof-of-concept measurements from OBLM studies into magnetrons at Teledyne e2v, Chelmsford. It also discusses design adjustments made to improve the detector sensitivity and how the performance can be enhanced using the sensor (or similar).

INTRODUCTION

Optical fibre-based beam loss monitors (OBLMs) consist of optical fibres running alongside a beamline, where at least one end of a fibre is monitored by a photodetector. OBLMs were first developed as a low-cost beam loss monitoring solution, with the capability for continuous accelerator coverage and approximately 0.5 m precision in the reconstruction of beam loss locations.

Beam losses are detected by monitoring relativistic secondary particle showers; produced when high-energy particles strike an obstacle such as the inside of the beam pipe [1]. The particle showers that intersect the optical fibre create a pulse of Cherenkov radiation inside it. [2] (Fig. 1). This radiation travels along the fibre and exits at the ends, where the photodetectors convert it into a voltage signal. The beam loss location can be reconstructed from the arrival time of the Cherenkov pulse [3]. A step-index silica fibre, with core diameter above 200 µm, is one type of optical fibre that is effective for this purpose. OBLMs are also sensitive to electrical arcing in radio-frequency (RF) accelerating cavities, also known as breakdown. Electrons emitted in the breakdown can be accelerated by the travelling RF wave in the cavity, and produce particle showers on striking the surface of the cavity or beam pipe [4]. Therefore, an OBLM system can be used to monitor both breakdowns and beam losses.

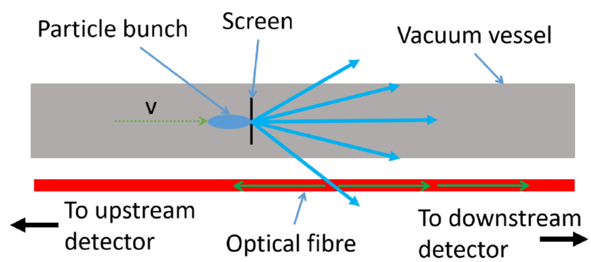

Figure 1: A diagram of the beam loss detection mechanism of the OBLM. Reproduced from [2] with permission.

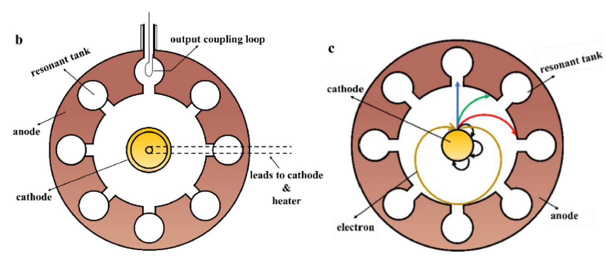

Figure 2: Cutaway view of a magnetron (b) and example electron paths within an operating magnetron (c) [6].

The applicability of this RF monitoring capability to magnetrons is the focus of this investigation. Magnetrons are a type of device that produces RF power, commonly used to power RF cavities of medical accelerators in addition to widespread use in radar and communications. During magnetron operation, a cloud of electrons rotates around the cathode in the central cavity, exciting standing RF waves in the resonant cavities [5] (Fig. 2). Since the maintenance of this electron cloud is largely reliant on the current of secondary electrons emitted from the cathode [6], damage to the cathode will reduce this current and degrade magnetron performance. Breakdowns are a common source of magnetron cathode damage – which itself increases the likelihood of further breakdowns. It is, therefore, useful to monitor breakdowns during magnetron operation in order to protect the device from unnecessary damage.

The proposed application of the OBLM was as an additional diagnostic for a magnetron test stand at Teledyne e2v (Chelmsford, UK), a leading magnetron manufacturer. Data from the OBLM and existing diagnostics could be used to train a machine learning (ML) model to predict breakdowns,

* This work is supported by STFC under grant ST/X000540/1), the Cockcroft Institute Core Grant (STFC ST/V001612/1) and the University of Liverpool Impact Acceleration Account.
† sgajon11@liverpool.ac.uk

ISBN: 978-3-95450-247-9 ISSN: 2673-5490 doi: 10.18429/JACoW-IPAC2024-WEPG16

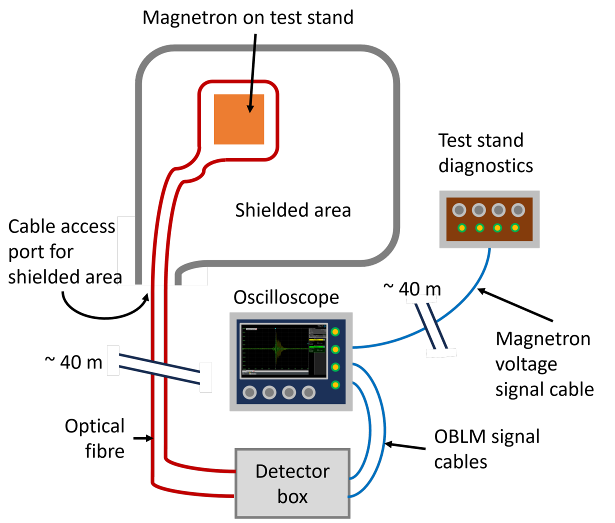

Figure 3: A representative diagram of the experimental setup at Teledyne e2v.

in a similar vein to a successful approach used in a study performed on the XBOX2 RF cavity test stand, at CERN [7]. However, proof-of-concept measurements were first required in order to verify that breakdowns in a magnetron were detectable in the OBLM system – since the minimum electron energy required for the production of Cherenkov light in a silica optical fibre of refractive index $n = 1.46$ is 186 keV [2]. Previous breakdown monitoring studies with the OBLM required high input power (above 10 MW) for the Cherenkov signal to be visible. However, the recent addition of new Onsemi J-Series silicon photomultiplier (SiPM) photodetectors to the OBLM system [8], along with bespoke power supply and amplification electronics, improved both the photon sensitivity and the rise/relaxation time by four orders of magnitude over the previous Hamamatsu Multi-Pixel-Photon-Counter (MPPC) SiPMs [2, 9]. This was expected to allow detection of lower-intensity Cherenkov signals that would likely be produced at lower input power.

PROOF OF CONCEPT MEASUREMENTS AT TELEDYNE E2V

The proof of concept measurements were carried out in November 2023 and March 2024 at Teledyne e2v. One step-index silica optical fibre was installed for this test, passing once around the magnetron and continuing outside of the shielded test area to reach the detector box containing two SiPM detectors - one monitoring each fibre end (Fig. 3).

The detector box was placed 40 m away from the test stand as part of measures taken to mitigate the effects of the high levels of electromagnetic interference (EMI) generated by the RF power switcher on the test stand; identified in the first testing run. These measures also included placing the photodetector box inside a Faraday cage of copper mesh, using ferrite rings to attenuate disturbances to the mains ground caused by breakdowns, and routing the detector output signals through double-screened cables. Some EMI still entered the system, but this was sufficiently reduced in post-processing with a 20 MHz low-pass digital filter.

During the tests, the magnetron was deliberately run in unfavourable conditions to provoke breakdowns, and the response of the OBLM system in comparison to signatures of breakdown was measured. The main signature was the sharp drop in magnetron voltage that occurs at the onset of breakdown. The magnetron voltage was recorded with the OBLM response data, in which it appears as a red line, but it was also recorded in the main test stand diagnostics to facilitate comparison between breakdown events recorded on each set of equipment. To probe the lower limit of input power usable with the OBLM system, the magnetron input power was increased approximately every 30 minutes if no obvious signals were visible in the SiPMs. The peak magnetron input power ranged from 4.470 MW to 6.281 MW, and the peak magnetron voltage ranged from 44.70 kV to its maximum of 48.96 kV (4s.f.).

Any Cherenkov radiation produced by a breakdown would be expected to be visible in both detectors. The lengths of the optical fibre sections and the cable carrying the magnetron voltage signal were used to estimate the expected delay between the arrival of the breakdown signal and the response signal of each SiPM to the arriving Cherenkov radiation. These delays were estimated as 130 ns for the first detector and 60 ns for the second detector. The length of fibre monitored by the first detector was approximately 14 m longer than the other, causing the additional delay. The lengths of the optical fibre sections were not precisely measured and were instead estimated to 1 s.f., limiting the precision of the calculated time delays.

SiPMs, in general, are known to exhibit background activity known as dark counts – where stochastic excitations can cause individual pixels to fire, producing a noise signal that forms the noise floor of the detector [10]. However, a single firing pixel produces a signal of characteristic height (known as a 1-photoelectron or 1 p.e. signal), allowing this noise to be removed using a threshold at 0.2 mV. Dark counts may also occasionally produce larger signals through the phenomenon of crosstalk, where the firing of one pixel has a probability of triggering others. The most common crosstalk event is a 2 p.e. signal, as higher-p.e. signals are often multiple orders of magnitude lower in probability. Comparisons with the expected signal delay times were used to remove the majority of dark count crosstalk signals, as this allowed the rejection of signals that were out of coincidence.

RESULTS

The main data set comprised 462 breakdown signatures. No signals above the 2 p.e. characteristic height were detected in this data set, which suggested that any Cherenkov signal present was close to the detector noise floor. A wide region of interest (1 µs before and after the breakdown signature) was chosen, and OBLM data sets that did not exceed the dark current rejection threshold in this region of interest were rejected from the analysis – reducing the number to

ISBN: 978-3-95450-247-9 ISSN: 2673-5490 doi: 10.18429/JACoW-IPAC2024-WEPG16

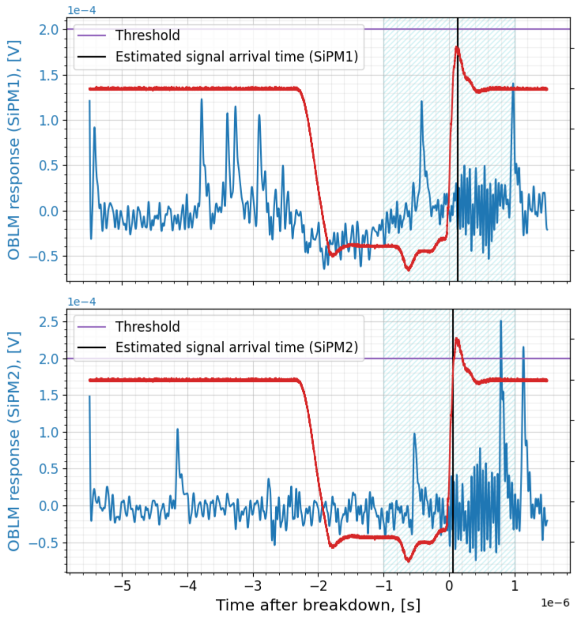

Figure 4: Comparison of the OBLM system response (after filtering) with the inverted magnetron voltage signal from one of the "Cherenkov detection candidate" data sets. The breakdown is estimated to occur at time zero, and the hatched area shows the initial (wide) region of interest. Dark counts can be seen throughout, particularly on the left-hand side of the top graph (SiPM 1). The peaks of interest – on the right-hand edge of the hatched area – are not close to the estimated signal arrival times.

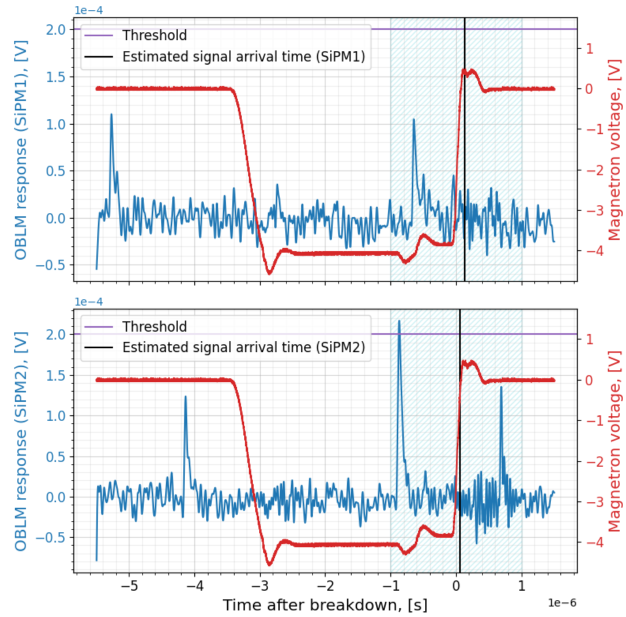

Figure 5: Comparison of of the OBLM system response (after filtering) with the inverted magnetron voltage signal, similar to Fig. 4. Two signal peaks, close in time, can be seen following a feature in the magnetron voltage occurring before the main "drop".

22 data sets. Three of these were rejected as their signals were dominated by EMI. Eight potential detection candidates were identified from the 19 remaining data sets, but none match the expected signal arrival times (Fig. 4).

The data suggests the following: either the OBLM system did not detect Cherenkov radiation from breakdowns in the magnetron and that the apparent signals are likely to be SiPM dark counts; or that the electrons emitted during breakdowns are less evenly distributed than first assumed. Agreement with the estimated signal arrival times would be expected for a uniform distribution; however, any directionality or other inhomogeneity would cause discrepancies between the signals at each fibre end.

Some further analysis, therefore, is required for sets of signals below the dark count threshold that fit with the expected arrival times – to determine their likelihood to be legitimate photon signals. Investigation into whether an OBLM signal is generated following features in the magnetron voltage signal that occur before the main voltage drop (as appears in Fig. 5) is also needed.

CONCLUSION

While the OBLM system has proven to be a useful tool for breakdown monitoring, a high input RF power (over 10 MW) was required for breakdowns to be detectable. The addition of the new detectors brought an increase in photon sensitivity which was hoped to reduce this input power requirement. An investigation was performed on a magnetron test stand at Teledyne e2v with peak input power exceeding 6 MW, probing the lower limits of input power usable with the OBLM system, but no obvious Cherenkov signals were detected in the expected time locations. This does not rule out Cherenkov detection from the results, but suggests that if the Cherenkov signal is present, it is close to the background; and that the electron distribution emitted from breakdowns is less uniform than first assumed. Further analysis is required to determine if Cherenkov detection events are present in the data. The mathematical description of Cherenkov radiation predicts the Cherenkov signals are likely to be more intense at higher electron energies [11], which may be achieved through higher voltages [12]. Additional research with RF devices capable of sustaining higher voltages than the 48.96 kV maximum achieved by the magnetron is therefore required.

REFERENCES

[1] A. Alexandrova *et al.*, "Optical beam loss monitor for RF cavity characterisation," 6th Int. Beam Instrumentation Conf. (IBIC'17), Grand Rapids, MI, USA, 20-24 August 2017, 2018, pp. 446–449. doi:10.18429/JACoW-IBIC2017-WEPWC01

[2] J. Wolfenden *et al.*, "Cherenkov radiation in optical fibres as a versatile machine protection system in particle accelerators," *Sensors*, vol. 23, no. 4, p. 2248, 2023, Number: 4 Publisher: Multidisciplinary Digital Publishing Institute. doi:10.3390/s23042248

ISBN: 978-3-95450-247-9 ISSN: 2673-5490 doi: 10.18429/JACoW-IPAC2024-WEPG16

[3] S. Benítez Berrocal *et al.*, "Beam loss localisation with an optical beam loss monitor in the CLEAR facility at CERN," *Proceedings of the 13th International Particle Accelerator Conference*, vol. IPAC2022, in collab. with Z. Frank (Ed.) *et al.*, p. 4, 2022. doi:10.18429/JACOW-IPAC2022-MOPOPT045

[4] M. Kastriotou *et al.*, "RF cavity induced sensitivity limitations on beam loss monitors," *Physics Procedia*, vol. 77, pp. 21–28, 1, 2015. doi:10.1016/j.phpro.2015.11.005

[5] "Magnetrons," in *Microwave and RF Vacuum Electronic Power Sources*, 2018, pp. 565–628. doi:10.1017/9780511979231.016

[6] Z. Liu, Y.-F. Yang, J.-H. Sun, H.-M. Liu, Z.-C. Li, and J.-S. Wang, "Cathodes in magnetrons: A review," *MetalMat*, vol. Early View, p. 10, e14 8, 2024, E-print: https://onlinelibrary.wiley.com/doi/pdf/10.1002/metm.14. doi:10.1002/metm.14

[7] C. Obermair *et al.*, "Explainable machine learning for breakdown prediction in high gradient rf cavities," *Physical Review Accelerators and Beams*, vol. 25, no. 10, p. 104 601, 4, 2022, Publisher: American Physical Society. doi:10.1103/PhysRevAccelBeams.25.104601

[8] onsemi. "J-series SiPM manufactured by semiconductor components industries, LLC," onsemi. (), https://www.onsemi.com/products/sensors/photodetectors-sipm-spad/silicon-photomultipliers-sipm/j-series

[9] A. Ghassemi, K. Sato, and K. Kobayashi, "MPPC SiPM manufactured by hamamatsu photonics k.k.," Hamamatsu Photonics K.K., Overview and explanation for MPPC sensors manufactured by Hamamatsu, 2022, p. 64. https://www.hamamatsu.com/content/dam/hamamatsu-photonics/sites/documents/99_SALES_LIBRARY/ssd/mppc_kapd9005e.pdf

[10] M. Kastriotou, "Optimisation of storage rings and RF accelerators via advanced fibre-based detectors," dphil, University of Liverpool, 2, 2018, 185 pp. https://livrepository.liverpool.ac.uk/3033777

[11] M. F. L'Annunziata, "Chapter 16 - cherenkov radiation," in *Radioactivity (Second Edition)*, 1, 2016, pp. 547–581. doi:10.1016/B978-0-444-63489-4.00016-2

[12] R. Appleby, G. Burt, J. Clarke, and H. Owen, *The Science and Technology of Particle Accelerators*. CRC Press, 28, 2020, 322 pp. doi:10.1201/9781351007962